ing group towards hydrolysis but does not behave as a redox catalyst. Such behavior appears to be unique to CAN.[13]

In summary, we have developed a highly efficient, catalytic protocol for the deprotection of acetals and ketals. This is the first time that such deprotections could be carried out under neutral to slightly basic conditions.

Experimental Section

Typical experimental procedure: Deprotection of 1,4-dioxadispiro-[4.0.5.3]tetradecan-7-one (Table 2, entry 6): Solid cerium ammonium nitrate (18 mg, 4 mol %) was added to a stirred solution of 1,4-dioxadispiro[4.0.5.3]tetradecan-7-one (237 mg, 1.13 mmol) in MeCN (3.5 mL) and borate–HCl buffer (Merck, pH 8, 3.5 mL). The faintly yellow solution was heated at 60 °C for 1.5 h. After cooling to room temperature, H_2O (10 mL) was added. The organic layer was separated, and the aqueous phase was extracted with CH_2Cl_2 (2×15 mL). The combined organic extracts were dried over $MgSO_4$ and filtered, and the solvents were removed in vacuo. The crude product was further purified by column chromatography on silica gel with EtOAc/hexane (3/7; $R_f = 0.58$) as the eluant. Spiro[4.5]decane-1,6-dione was obtained as a colorless liquid (144 mg, 86 %). ^{1}H NMR ($CDCl_3$, 300 MHz): $\delta = 2.7$ (m, 2H), 2.42 (dt, $J = 14.1$, 5.1 Hz, 1H), 2.31 (dt, $J = 8$, 1.7 Hz, 2H), 2.2 to 1.6 (m, 9H); ^{13}C{^{1}H} NMR ($CDCl_3$, 75.5 MHz): $\delta = 18.9$, 21.0, 26.6, 33.7, 35.9, 38.4, 39.7, 64.3, 207.9, 215.5; IR (film): $\tilde{\nu} =$ 1734, 1700 cm^{-1}; MS (70 eV): *m/z* (%): 166 (92) [M^+], 167 (100) [M^++1].

Received: March 17, 1999
revised version: July 19, 1999 [Z 13181 IE]
German version: *Angew. Chem.* **1999**, *111*, 3411–3413

Keywords: aldehydes · cerium · homogeneous catalysis · ketones · protecting groups

[1] a) P. J. Kocienski in *Protecting Groups*, Thieme, New York, **1994**; b) T. W. Greene, P. G. M. Wuts in *Protective Groups in Organic Chemistry*, Wiley, New York, **1991**.
[2] Selected references: a) C. E. Ballou, H. O. L. Fischer, *J. Am. Chem. Soc.* **1956**, *78*, 1659–1661; b) A. J. Showler, P. A. Darley, *Chem. Rev.* **1967**, *67*, 427–440; c) A. S. Y. Lee, C. L. Cheng, *Tetrahedron* **1997**, *53*, 14255–14262, and references therein.
[3] A. Ates, PhD Thesis, Université catholique de Louvain, in preparation.
[4] The sensitivity of this aldol product **2** towards acidic conditions is further illustrated by its complete transformation into **3** during attempted purification by chromatography on silica gel.
[5] A. Ates, A. Gautier, B. Leroy, J. M. Plancher, Y. Quesnel, I. E. Markó, *Tetrahedron Lett.* **1999**, *40*, 1799–1802.
[6] a) T. L. Ho, "Cerium(IV) Oxidation of Organic Compounds" in *Organic Synthesis by Oxidation with Metal Compounds* (Eds.: W. J. Mijs, C. R. H. I. de Jonge), Plenum Press, New York, **1986**; b) J. R. Hwu, M. L. Jain, S. C. Tsay, G. H. Hakimelahi, *Tetrahedron Lett.* **1996**, *37*, 2035–2038, and references therein.
[7] a) T. L. Ho, *Synthesis* **1978**, 936; b) G. A. Olah, B. G. B. Gupta, A. P. Fung, *Synthesis* **1980**, 897–898; c) H. Tomioka, K. Oshima, H. Nozaki, *Tetrahedron Lett.* **1982**, *23*, 539–542.
[8] So far, we have not been able to find reaction conditions under which unmasking of a dioxolane group could be accomplished chemoselectively in the presence of a *tert*-butyldimethylsilyl (TBDMS) protecting group.
[9] In the presence of $NaBrO_3$, competitive oxidation to give the 2-hydroxyethyl ester derivative takes place.
[10] With 2.5 equivalents of CAN, epimerization takes place, affording a near thermodynamic mixture of axial and equatorial product (60:40).
[11] Deprotection of ketal **6** with 2.5 equivalents of CAN resulted in quantitative formation of *tert*-butylcyclohexanone. However, no 1,2-octanediol could be isolated in this experiment. In contrast, removal of the dioxolane protecting group with 3 mol % CAN in borate buffer (pH 8) afforded not only the desired ketone (95 %) but also 1,2-octanediol (97 %); hence, a different mechanism operates in these two reactions.
[12] Chemoselective deprotections can thus be realized by using dioxolane protecting groups with different steric demands.
[13] Indeed, $Ce(NO_3)_3$, $Ce(OTf)_4$, and other lanthanide salts were inert under our reaction conditions.

Fluorescent Indicators for Imaging Nitric Oxide Production**

Hirotatsu Kojima, Yasuteru Urano, Kazuya Kikuchi, Tsunehiko Higuchi, Yasunobu Hirata, and Tetsuo Nagano*

Nitric oxide (NO) is a signal transmitter in vivo.[1] However, many of the functions proposed for NO remain controversial owing to the lack of direct evidence. The use of NO-reactive fluorescent indicators which allow bioimaging of NO with high spatial and temporal resolution in conjunction with fluorescence microscopy should overcome this problem. A reaction that traps NO directly is essential for developing probes for NO, but NO itself shows low reactivity towards organic compounds. Further, a nitroso or nitro group will generally quench fluorescence when dyes react with NO to generate these functional groups. Therefore, few reactions are suitable for this purpose. Recently, fluorescent probes for NO, FNOCTs, were reported.[2] They react with NO to yield nonfluorescent compounds that are reduced by biological compounds, such as ascorbic acid, to afford fluorescent derivatives. However, they have not yet been applied in biological experiments.

We have developed diaminofluoresceins (DAFs), such as DAF-2 (Scheme 1), as fluorescent indicators for NO.[3, 4] The DAFs react not with NO itself but with NO^+ equivalents, such as nitric anhydride (N_2O_3), which are formed by autoxidation of NO. Under aerobic conditions, DAFs can trap NO to yield highly fluorescent triazolofluoresceins (DAF-Ts) by nitrosation and dehydration. This mechanism is convenient because it does not interfere with signal transduction, but is

[*] Prof. T. Nagano, H. Kojima, Dr. Y. Urano, Dr. K. Kikuchi, Dr. T. Higuchi
Graduate School of Pharmaceutical Sciences
The University of Tokyo
7-3-1 Hongo, Bunkyo-ku, Tokyo 113-0033 (Japan)
Fax: (+81) 3-5841-4855
E-mail: tlong@mol.f.u-tokyo.ac.jp
Dr. Y. Hirata
The Second Department of Internal Medicine, Faculty of Medicine
The University of Tokyo (Japan)

[**] This work was supported by JSPS Research Fellowships for Young Scientists and by Grants-in-Aid for Scientific Research on Priority Areas nos. 09304061, 10169215, and 10557243 from the Ministry of Education, Science, Sport, and Culture of Japan. The authors are indebted to M. Morita for advice on the preparation of bovine aortic endothelial cells.

Supporting information for this article is available on the WWW under http://www/wiley-vch.de/home/angewandte/ or from the author.

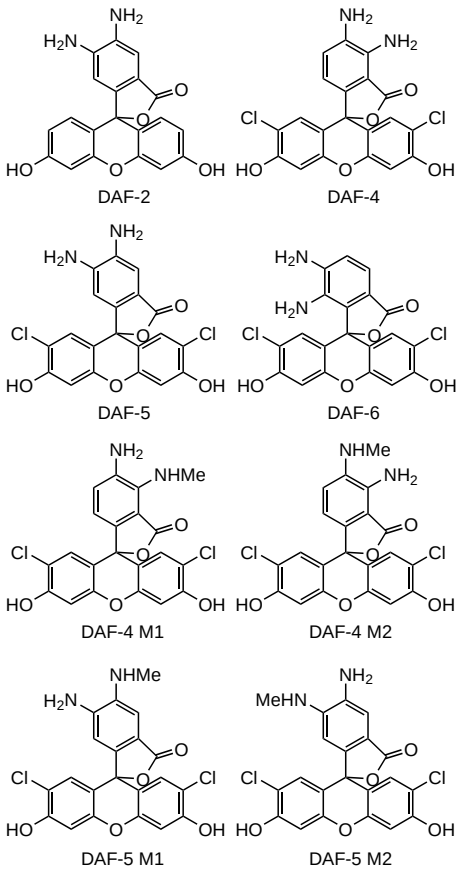

Scheme 1. Chemical structures of the fluorescent NO indicators. DAF-2 and DAF-4 were previously reported.[3]

disadvantageous from the viewpoint of sensitivity. Under physiological conditions, DAF-Ts are not formed in the absence of NO, which is why DAFs can be used for direct detection of NO produced by cells. However, during the application of DAF-2 for NO imaging in vascular endothelial cells, we encountered the problem of pH dependency of the fluorescence intensity of DAF-Ts, which makes it difficult to monitor small changes in intracellular NO levels after a stimulus that shifts the intracellular pH level. For example, it was reported that stimulation with bradykinin lowers the pH value in vascular endothelial cells to 6.5.[5] Since we had anticipated this problem, we synthesized dichloro derivatives of DAF (DAF-4, DAF-5, and DAF-6; Scheme 1).

The chlorine atoms lower the pK_a value of the adjacent phenolic OH group due to their electronegativity. However, they were unexpectedly less useful than DAF-2 owing to their unstable fluorescence intensity around neutral pH. The instability may arise from a triazole proton, so we introduced a methyl group (DAF-4 M1, DAF-4 M2, DAF-5 M1, and DAF-5 M2; Scheme 1). Derivatives of DAF-6 were not synthesized due to the low chemical yield and the low sensitivity of DAF-6 in comparison with DAF-1 – DAF-5. The sensitivities of these new dyes to NO were determined by using the NO-releasing compound NONOate.[6] After 1 h of incubation at 37 °C with NONOate (half-life: 13.7 min at 22 °C), the fluorescence intensity at the appropriate wavelengths of 10 μM DAF-4, DAF-5, DAF-4 M1, DAF-4 M2, DAF-5 M1, and DAF-5 M2 increased by 380, 339, 75, 417, 195, and 196 units, respectively. Thus, DAF-4 M2 was the most sensitive to NO. The fluorescence intensity of the triazole form of DAF-4 M2 was stable above pH 5.8.

It was reported that fluorinated fluorescein derivatives are more resistant to photobleaching than fluorescein and can be efficiently excited with the 488-nm spectral line of the argon-ion laser used in confocal laser scanning microscopes.[7] Therefore, we prepared DAF-FM (Scheme 2), in which the

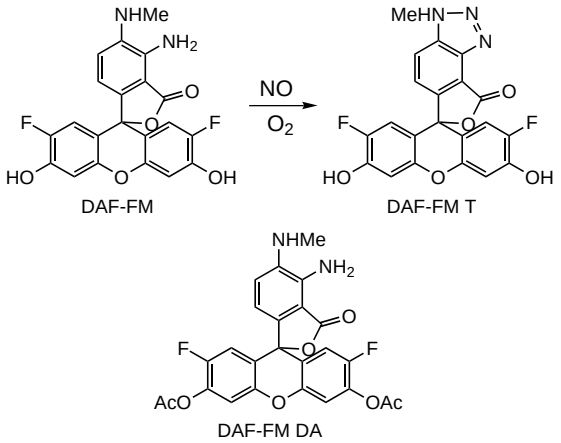

Scheme 2. Structures of fluorinated DAFs, and the synthesis of the triazole form DAF-FM T.

chlorine atoms of DAF-4 M2 are replaced by fluorine atoms. Photobleaching was examined in sunlight. The fluorescence intensity of the triazole form of DAF-FM (DAF-FM T) was reduced to 94, 63, and 28% of the initial intensity after 1, 2, and 3 h, respectively, while that of DAF-2 T decreased to 58, 11, and 1%, and that of DAF-4 T to 81, 45, and 20%.

The effect of pH on the fluorescence intensity of DAF-FM T was also examined. The pK_a value of the phenolic OH group of DAF-FM was 4.38 ± 0.05. The fluorescence intensity was stable above pH 5.8 (Figure 1). The absorbance and

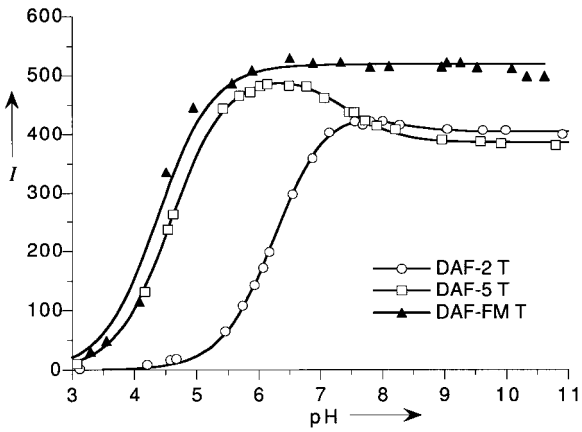

Figure 1. Effect of pH on the fluorescence intensity I of DAF-Ts. Triazole forms of DAF-2, DAF-5, and DAF-FM (1 μM) were added to sodium phosphate solution adjusted to various pH values. The pH was measured after mixing. The fluorescence intensities of DAF-2T, DAF-5T, and DAF-FMT were determined at 515, 520, and 515 nm with excitation at 495, 505, and 495 nm, respectively. The curves were fitted to the following equations: DAF-2T: $I = 460/(1+10^{6.27-pH}) - 55.6/(1+10^{7.94-pH})$, $R = 1.00$; DAF-5T: $I = 505/(1+10^{4.59-pH}) - 119/(1+10^{7.41-pH})$, $R = 1.00$; DAF-FM T: $I = 518/(1+10^{4.38-pH})$, $R = 0.994$.

  1433-7851/99/3821-3210 $ 17.50+.50/0

fluorescence properties of the DAFs are summarized in Table 1. As expected, the peak wavelengths of DAF-FM do not differ from those of DAF-2, unlike those of DAF-4. The augmentation of the fluorescence intensity of DAF-FM upon addition of NO is shown in Figure 2. Judging from NO standard curves calibrated with 7 μM DAF-FM, the detection limit of NO was 3 nM. The sensitivity of DAF-FM was 1.4 times higher than that of DAF-2. It is considered that this increase in sensitivity results from the higher rate of the reaction with NO^+ equivalents due to the electron-donating effect of the methyl group.

Table 1. Absorbance and fluorescence properties of dyes.[a]

Dye	Extinction coefficients [$\times 10^4$ M^{-1}cm^{-1}], absorption maxima [nm]		Fluorescence maximum of triazole form [nm]	Relative quantum efficiencies	
	diamine	triazole		diamine	triazole
DAF-2	7.9, 486	7.3, 491	513	0.005	0.92
DAF-4	9.7, 501	9.2, 505	530	0.002	0.75
DAF-FM	8.4, 487	7.3, 495	515	0.005	0.81

[a] All data were obtained at 20 °C in 0.1 M sodium phosphate buffer (pH 7.4).

For the bioimaging of NO, we synthesized DAF-FM DA (Scheme 2), which permeates well into cells and is quickly transformed into water-soluble DAF-FM by esterases in the cytosol, where the dye can remain for a long time. The indicator DAF-FM DA was applied to the imaging of NO in cultured bovine aortic endothelial cells by using a fluorescence microscope. The cells were incubated with 10 μM DAF-FM DA for 1 h at 37 °C for dye loading. The fluorescence images before and after stimulation of the cells with 0.1 μM bradykinin are shown in Figure 3. Line A in Figure 4 shows the corresponding data. After stimulation, the fluorescence intensity in the cells increased, and that in the cytosol increased more than that in the nucleus. Nitric oxide is believed to be produced in the cytosol, where NO synthase exists. This observation implies that little of the produced NO diffuses into the nucleus, or, if it does diffuse into the nucleus, little of it is oxidized there. Line B in Figure 4 shows the control data, for which the augmentation of the fluorescence intensity was suppressed by the NO synthase inhibitor L-nitroarginine methyl ester (L-NAME).

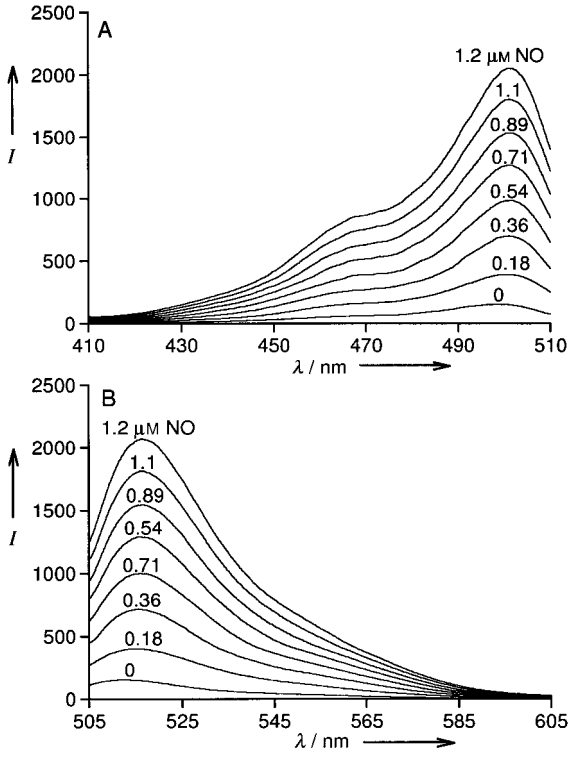

Figure 2. Excitation (A) and emission (B) spectra of DAF-FM at 37 °C in 0.1 M sodium phosphate buffer (pH 7.4) with NO concentrations ranging from 0 μM to 1.2 μM. A solution of NO was added to 7 μM DAF-FM solution under aerobic conditions. The spectra were obtained from an average of five repeated measurements 15 min after the addition of NO solution. A) Determined with emission at 515 nm. B) Determined with excitation at 500 nm.

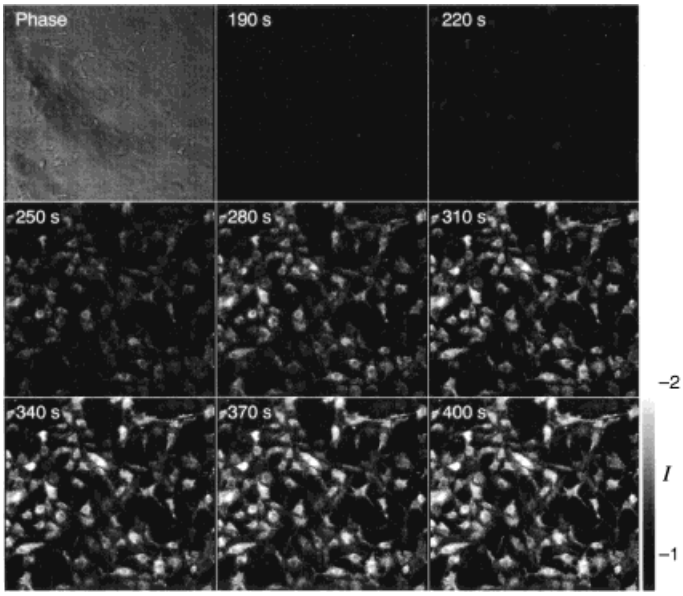

Figure 3. Bright-field and fluorescence images of cultured bovine aortic endothelial cells loaded with DAF-FM DA. Times from the start of measurement are shown. At 200 s, bradykinin (0.1 μM) was added. The fluorescence images are shown as ratio images on the basis of the initial intensity at the start of measurement and correspond to the fluorescence intensity data in Figure 4 (line A).

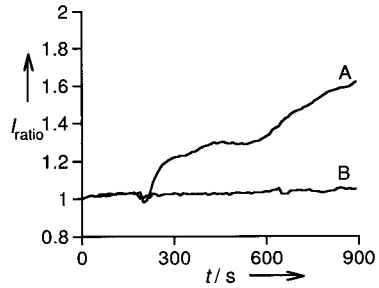

Figure 4. Fluorescence response of DAF-FM DA-loaded cultured bovine aortic endothelial cells, reflecting NO production in response to the addition of 0.1 μM bradykinin at 200 s. Fluorescence was measured at 10-s intervals. A) Ratio of fluorescence intensity I_{ratio} of the cells corresponding to Figure 3. B) Ratio of fluorescence intensity of the cells in the presence of the NO synthase inhibitor L-NAME (1 mM). The lines show mean values of the average fluorescence intensity in seven areas containing a cell.

  1433-7851/99/3821-3211 $ 17.50+.50/0

In conclusion, we suggest that DAF-FM is a useful tool for visualizing the temporal and spatial distribution of intracellular NO.

Experimental Section

The synthesis of the indicators is described in the Supporting Information.

Fluorescence spectroscopy: The DAFs were dissolved in DMSO to obtain 10 mM stock solutions. Relative quantum efficiencies of fluorescence of DAFs and DAF-Ts were obtained by comparing the area under the corrected emission spectrum of the test sample upon excitation at 492 nm with that of a solution of fluorescein in 0.1 M sodium hydroxide, which has a quantum efficiency of 0.85.[8] Bleaching of dyes (10 μM) was determined in 0.1 M sodium phosphate buffer (pH 7.4). The solutions in 30-mL vials were placed in full sunlight on a fine day in November in Tokyo and were sampled every 1 h.

Imaging: Primary cultured endothelial cells from bovine aorta were passaged in Dulbecco's modified Eagle's medium containing 10% fetal bovine serum and antibiotics. Cells between the 13th and 16th passages were used for these experiments. The cells were incubated for 1 h at 37 °C in PBS(+) (PBS = phosphate buffered saline) containing 10 μM DAF-FM DA (0.2% DMSO) for loading, and washed with PBS(+). They were mounted on an inverted fluorescence microscope (Olympus IX70, Tokyo, Japan) equipped with an objective lens (×20), an excitation filter (490 nm), a dichroic mirror (505 nm), and a long-pass emission filter (515 nm). The air temperature was maintained at 37 °C with a warming box (IX-IBM, Olympus). Optical signals were recorded with an Argus 50 (Hamamatsu Photonics, Shizuoka, Japan), which is an imaging system including a cooled charge-coupled device (CCD) camera. Bradykinin and L-NAME were purchased from Sigma (St. Louis, MO, USA).

Received: May 10, 1999 [Z13402IE]
German version: *Angew. Chem.* **1999**, *111*, 3419 – 3422

Keywords: dyes · fluorescence spectroscopy · nitrogen monoxide · sensors · signal transduction

[1] *Methods Enzymol.* **1996**, *269* (the reference refers to the whole issue).
[2] M. Bätz, H. G. Korth, R. Sustmann, *Angew. Chem.* **1997**, *109*, 1555 – 1557; *Angew. Chem. Int. Ed. Engl.* **1997**, *36*, 1501 – 1503.
[3] H. Kojima, N. Nakatsubo, K. Kikuchi, S. Kawahara, Y. Kirino, H. Nagoshi, Y. Hirata, T. Nagano, *Anal. Chem.* **1998**, *70*, 2446 – 2453.
[4] N. Nakatsubo, H. Kojima, K. Kikuchi, H. Nagoshi, Y. Hirata, D. Maeda, Y. Imai, T. Irimura, T. Nagano, *FEBS Lett.* **1998**, *427*, 263 – 266.
[5] I. Fleming, M. Hecker, R. Busse, *Circ. Res.* **1994**, *74*, 1220 – 1226.
[6] NONOate = (*Z*)-1-{*N*-[3-aminopropyl]-*N*-[4-(3-aminopropylammonio)butyl]amino}diazen-1-ium-1,2-diolate; see: J. A. Hrabie, J. R. Klose, D. A. Wink, L. K. Keefer, *J. Org. Chem.* **1993**, *58*, 1472 – 1476.
[7] W. C. Sun, K. R. Gee, D. H. Klaubert, R. P. Haugland, *J. Org. Chem.* **1997**, *62*, 6469 – 6475.
[8] Y. Nishikawa, K. Hiraki, *Analytical Methods of Fluorescence and Phosphorescence*, Kyoritsu Publishing Company, Tokyo, **1984**, pp. 76 – 80.

Ferrocenyl Ligands with Two Phosphanyl Substituents in the α,ε positions for the Transition Metal Catalyzed Asymmetric Hydrogenation of Functionalized Double Bonds**

Tania Ireland, Gabriele Grossheimann, Catherine Wieser-Jeunesse, and Paul Knochel*

Dedicated to Professor Armin de Meijere on the occasion of his 60th birthday

Chiral ferrocene ligands have found numerous useful applications in asymmetric catalysis.[1] Recently, we described a new family of C_2-symmetrical ferrocenyl ligands called Ferriphos **1**, which proved to be efficient catalysts for the hydrogenation of α-acetoamidoacrylic acid derivatives.[2, 3] We have now discovered another class of chiral diphosphanylferrocenyl derivatives **2a**–**d** which are excellent ligands for the enantioselective hydrogenation of various functionalized double bonds and carbonyl groups. The relatively broad area

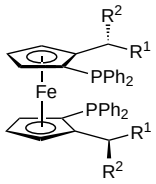

1: Ferriphos

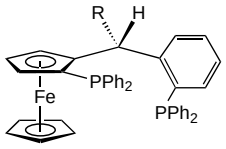

2a : R = NMe_2
2b : R = *N*-pyrrolidyl
2c : R = Me
2d : R = *i*Pr

of application of this new class of α,ε-diphosphanes in asymmetric catalysis as well as their short synthesis makes these ligands especially attractive. The modular approach to their synthesis means that a variety of substituents R (alkyl or amino groups) can be introduced in the benzylic position. As shown later, the nature of R is crucial to the enantioselectivity observed with these ligands.

The ferrocenyl derivatives **2** are readily prepared in five steps starting from ferrocene (Scheme 1). Thus, a Friedel – Crafts acylation of ferrocene with 2-bromobenzoyl chloride furnishes the ferrocenyl ketone **3** in 80% yield. The Corey-Bakshi-Shibata (CBS) reduction[4] of **3** affords the corresponding ferrocenyl alcohol in 95% yield and 96% *ee*. This

[*] Prof. Dr. P. Knochel, Dipl.-Chem. T. Ireland, Dr. G. Grossheimann, Dr. C. Wieser-Jeunesse
Fachbereich Chemie der Universität
Hans-Meerwein-Strasse, D-35032 Marburg (Germany)
and
Institut für Organische Chemie der Universität
Butenandtstrasse 5 – 13, D-81377 München (Germany)
Fax: (+49) 89-2180-7680
E-mail: Paul.Knochel@cup.uni-muenchen.de

[**] We thank the DFG (SFB 260, Graduiertenkolleg, Leibniz-Programm) and the Fonds der Chemischen Industrie for financial support. We thank Dr. Klaus Harms for the crystal structure analysis as well as Degussa-Hüls AG and Chemetall GmbH for the generous donation of chemicals. C.W.-J. thanks the Alexander-von-Humboldt-Stiftung for a stipendium.

  1433-7851/99/3821-3212 $ 17.50+.50/0